Wavelet-based analysis of EEG signals for detection and localization of epileptic seizures

George Benke*, Maribeth Bozek-Kuzmicki, David Colella, Garry M. Jacyna, John J. Benedetto**

The MITRE Corporation, Signal Processing Center
7525 Colshire Drive, McLean VA. 22102
* also with the Department of Mathematics, Georgetown University
** also with the Department of Mathematics, University of Maryland

ABSTRACT

A wavelet-based technique WISP is used to discriminate normal brain activity from brain activity during epileptic seizures. The WISP technique is used to exploit the noted difference in frequency content during the normal brain state and the seizure brain state so that detection and localization decisions can be made. An AR-Pole statistic technique is used as a comparative measure to base-line the WISP performance.

Keywords: EEG, ECoG, epileptic seizures, wavelets, AR Models, WISP, detection, localization

1. INTRODUCTION

This paper deals with the analysis of electrical potential time series derived from brain activity of patients with epilepsy.[1,2] The goal is to develop analytical methods and algorithms which detect the presence of a seizure (the detection problem) and which identify the regions of the brain which cause the seizure (the localization problem). It has not been established that there is always a well-defined cortical focus which is responsible for the initiation of a seizure. Nevertheless, current surgical treatment for certain forms of epilepsy seeks to remove a minimal amount of brain tissue responsible for the onset of seizures. The most common signals derived from brain potentials are electroencephalograms (EEGs). Since these signals are measured on the scalp and potentials are on the order of microvolts, these signals are subject to many complicated influences such as head geometry, propagation through holes in the skull, muscle movement, etc. These effects are often regarded as "noise" and, consequently, the signal-to-noise ratio of EEG time series is low. Time series which have a much higher signal-to-noise ratio are obtained by measuring potentials directly on the surface of the brain. These are called electrocorticograms (ECoGs) and can only be obtained by much more invasive procedures. Figure 1 shows EEG and ECoG recordings from the same individual during different time epochs.

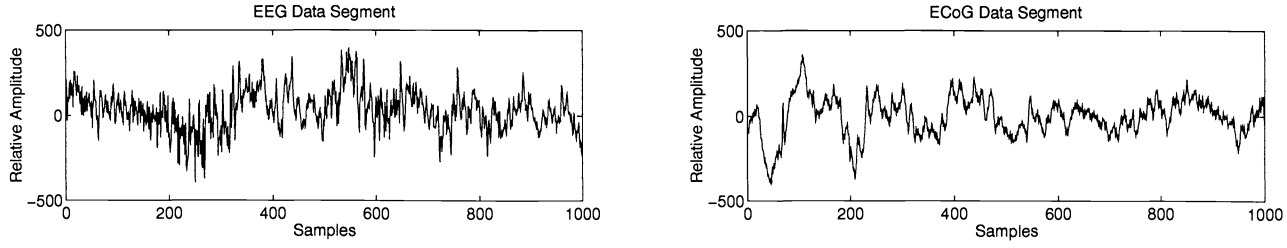

(a) (b)

Figure 1: Comparison of EEG (a) and ECoG (b) recordings from the same patient

0-8194-1844-7/95/$6.00

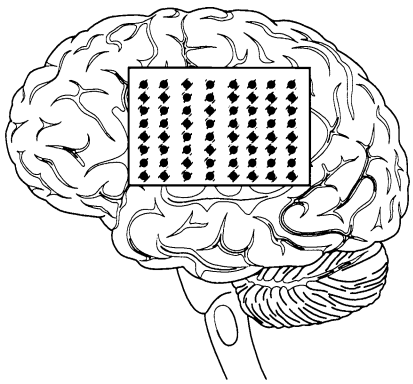

Figure 2: Illustration depicting an electrode grid on the brain surface

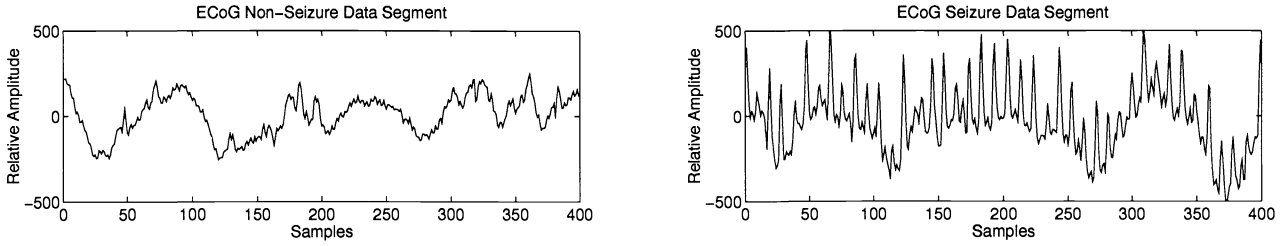

(a) (b)

Figure 3: Examples of ECoG Non-Seizure (a) and Seizure Data (b) Segments

Localization of a seizure focus is often accomplished by multi-channel processing of a matrix ECoG time series derived from surface electrodes (see Figure 2). The work described in this paper is based on the analysis of ECoG time series data consisting of 64 channels recorded by an 8x8 block of electrodes spaced approximately 1 cm apart. Figure 3 shows typical recorded waveforms during non-seizure activity and seizure activity, respectively.

A standard method for seizure localization is a manual time-difference-of-arrival analysis. Here one (visually) identifies regions of early onset and propagation of seizure activity across the grid. As shown in Figure 4, onset of seizure activity is first apparent in channel 9. Next, the seizure activity spreads to neighboring channels 10 and 11 and in the end appears in most, if not all, of the recorded waveforms. In this paper we examine two signal analysis techniques and their efficacy for analyzing ECoG data. The first technique, which we call *wavelet integer scale processing* (WISP), gives a time-scale representation of the signal. The second technique produces a time series-based statistic which measures the pole configuration of a local autoregressive (AR) model of the data. We will show how both of these techniques find a certain feature of the data which is useful for both the detection and localization problems.

The paper is organized as follows. In Section 2 we review the nature of the data and some of its important features. In Section 3 we describe the WISP technique and show some typical results of ECoG data analysis using this technique. In Section 4 we describe the AR-pole statistic and the results produced by this type of analysis. In Section 5 we summarize processing results and in Section 6 we draw some conclusions concerning these and other techniques for the analysis of ECoG data.

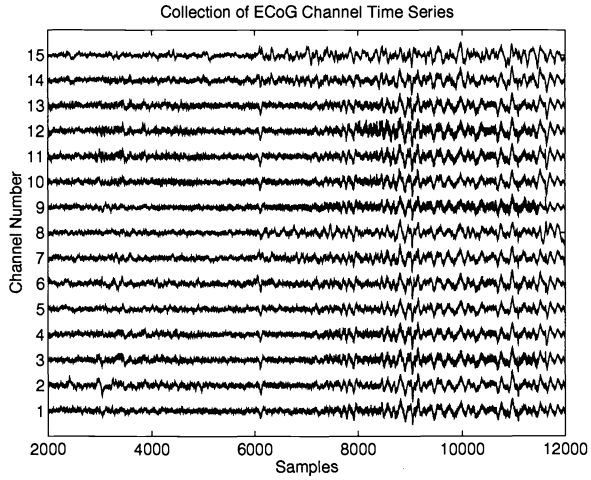

Figure 4: 15 ECoG channels showing the difference in seizure arrival times

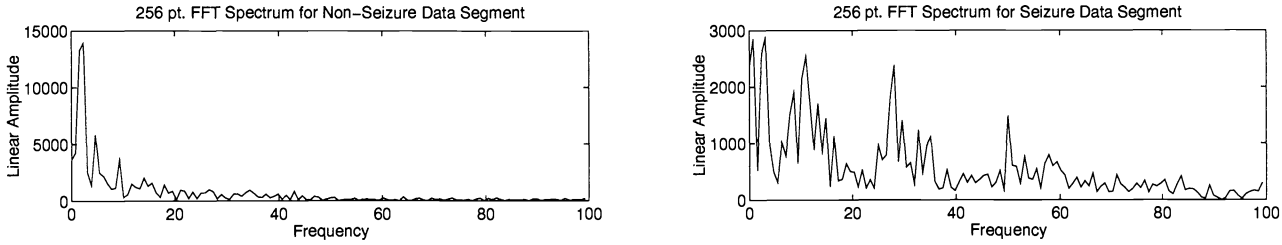

(a) (b)

Figure 5: FFT Spectrums of ECoG Non-Seizure (a) and Seizure (b) Data Segments

2. ECoG RECORDINGS

The two plots in Figure 3 show clear structural differences in the two classes of data, non-seizure and seizure, sampled at 200 Hz. The signal in Figure 3(a), which corresponds to normal brain activity, is clearly of lower energy than the signal in Figure 3(b), which corresponds to a seizure in progress. In terms of spectral structure there is also a fairly clear distinction. The spectrum of the signal during normal activity tends to have a fractal (1/f-like) spectrum, while during a seizure there are harmonic peaks which suggest that a fairly simple dynamical system is in resonance (see Figure 5).

Further spectral analysis of the signal during seizure shows that the harmonic peaks drift toward lower frequencies as the seizure progresses and finally collapse as the seizure ends. It is not unreasonable to speculate that some chemical, perhaps a neurotransmitter, is being depleted as the seizure progresses until finally there is not enough to sustain the resonance of the dynamical system.

It should also be observed that during the transition period between normal brain activity and the seizure the ECoG potential signal drops significantly. In the neurophysiology literature this epoch of reduced amplitude activity is referred to as the electrodecremental period. An illustration of the electrodecremental

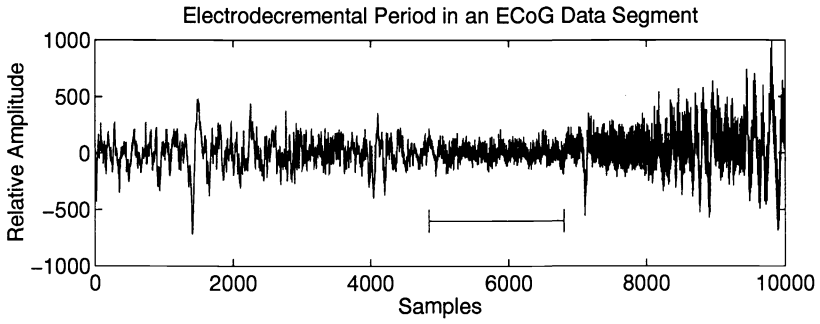

Figure 6: Example of the Electrodecremental Period in ECoG Recordings.

period is indicated by the horizontal bar marking for the time series shown in Figure 6. During this period there is also an increase in high frequency activity, although the harmonic peaks are not as yet well defined. The two methods discussed in this paper, WISP and a low-order autoregressive model, attempt to exploit this spectral difference between non-seizure and seizure data by looking for particular harmonic structures.

3. WISP PROCESSING

The wavelet integer scale processing algorithm is derived from the continuous wavelet transform in that it redundantly samples a continuous wavelet transform of a signal in both scale and time. For our purposes here we consider the "square" wavelet

$$h(t) = \begin{cases} \dfrac{1}{\sqrt{2\pi}} & ,0 < t < \pi \\ -\dfrac{1}{\sqrt{2\pi}} & ,-\pi < t < 0 \end{cases}$$

where for any $f \in L^2(\mathbf{R})$ the wavelet transform is given by

$$Wf(a,b) = \int_{-\infty}^{\infty} \frac{1}{\sqrt{a}} h\left(\frac{t-b}{a}\right) f(t)dt,$$

with $a > 0$ and $b \in \mathbf{R}$. In the application of WISP to a sampled time series, the resulting output is essentially a sampled continuous wavelet transform where now a, b assume discrete values. We are primarily concerned with sampled ECoG and EEG data. Although we present the WISP processing methodology in the continuous setting for simplicity, modifications for the processing of sampled data are left to the reader.

Since our data suggests the existence of spectral peaks, let us examine the (continuous) wavelet transform of a pure frequency component. Suppose $f(t) = \sin(\gamma t + \phi)$ for a fixed γ and ϕ. Then

$$
\begin{aligned}
Wf(a,b) &= \int_{b-\pi a}^{b} \frac{-1}{\sqrt{2a\pi}} \sin(\gamma t+\phi)dt + \int_{b}^{b+\pi a} \frac{1}{\sqrt{2a\pi}} \sin(\gamma t+\phi)dt \\
&= \frac{1}{\gamma\sqrt{2a\pi}} \left[\cos(\gamma b+\phi) - \cos(\gamma(b-\pi a)+\phi) - \cos(\gamma(b+\pi a)+\phi) + \cos(\gamma b+\phi)\right] \\
&= \frac{4}{\gamma\sqrt{2a\pi}} \cos(\gamma b+\phi) \sin^2\left(\frac{\gamma\pi a}{2}\right).
\end{aligned}
$$

Note that if $a = \dfrac{2k+1}{\gamma}$ for some integer k, then

$$
Wf(a,b) = (-1)^k \frac{4}{\sqrt{2\pi(2k+1)\gamma}} \cos(\gamma b+\phi).
$$

This shows that at scales a which are odd multiples of $1/\gamma$, the wavelet transform of f varies in time variable b like a pure sinusoid of frequency $\gamma/2\pi$. An examination of the scaleograms in Figure 7 reveals sinusoidal behavior at certain scales for seizure data and the marked absence of these sinusoidal components for non-seizure data. The scaleogram in Figure 7(b) indicates the presence of sinusoids at five or six different scales that appear linearly related. The linearity relative to scale is consistent with the fact that the sampling of the continuous wavelet transform is linear. Translating the scales into frequencies, we find that the scalogram in Figure 7(b) indicates sinusoidal components at frequencies roughly equal to 15, 30, 45, 60, 75, and 90 Hz (keep in mind that the Nyquist frequency is 100 Hz). Althought this paper does not address the possible models that would give rise to output as in Figure 7(b), the sinusoidal output associated with this seizure activity is consistent with a relatively simple dynamical system that has been outlined in an earlier paper.[3]

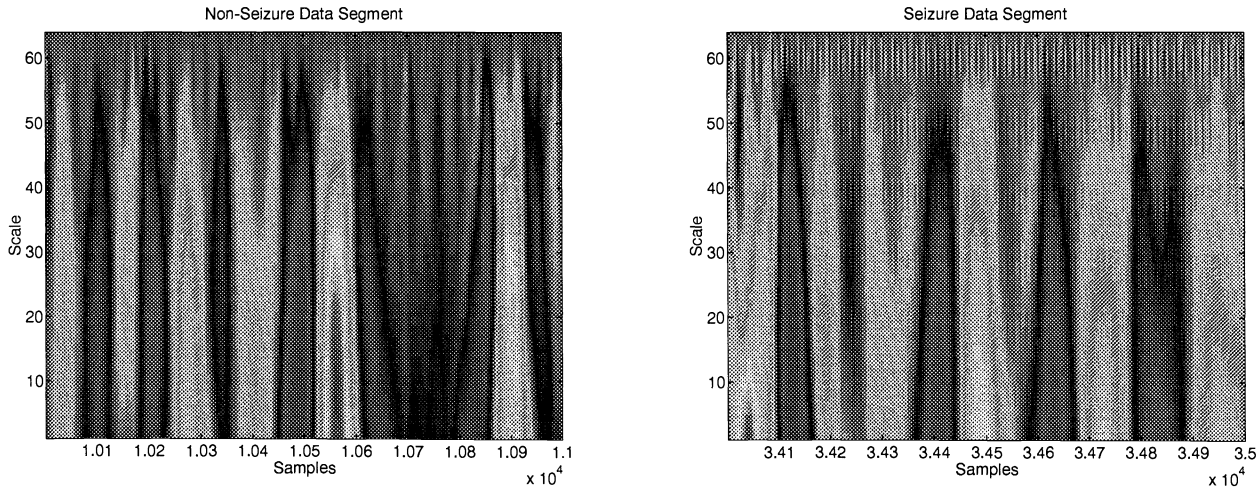

(a) (b)

Figure 7: WISP output for a Non-Seizure Data Segment (a) and a Seizure Data Segment (b)

4. THE AR-POLE STATISTIC

Given discrete time series data x_n we now consider a standard autoregressive model

$$x_n = \sum_{k=1}^{p} a_k x_{n-k} \tag{1}$$

of order p. For a particular window of data x_m, x_{m+1}, ..., x_{m+n-1} consisting of n contiguous samples, we seek the a_k's which give the best least-squares fit of our model to the data in the processing window.[4] That is, if $F = \{m, ..., m+n-1\}$, we seek the a_k's which minimize

$$\sum_{n \in F} \left| x_n - \sum_{k=1}^{p} a_k x_{n-k} \right|^2 .$$

Since this expression is quadratic in the a_k's, it is minimized by solving a symmetric system of linear equations. Since Equation (1) is satisfied exactly if and only if the data x_n is a linear combination of exponentials (or exponentials multiplied by polynomials), for real time series data the "prediction error"

$$e_n = x_n - \sum_{k=1}^{p} a_k x_k \tag{2}$$

will not be zero on all of F. Taking the z-transform of Equation (2) gives

$$E(z) = P(z^{-1})X(z) , \tag{3}$$

where E and X are the z-transforms of e_n and x_n, respectively, and P is the polynomial

$$P(z) = 1 - \sum_{k=1}^{p} a_k z^k .$$

It therefore follows from Equation (3) that the z-transform of x_n is

$$X(z) = \frac{1}{P(z^{-1})} E(z)$$

and the Fourier transform of x_n is

$$X(e^{iw}) = \frac{1}{P(e^{-iw})} E(e^{iw}) . \tag{4}$$

The model (1) is reasonable if the prediction error e_n is '"noise like," which means that it should have a relatively flat spectrum. Equation (4) therefore shows that sharp spectral peaks of x_n are closely related to the existence of zeros of P near the unit circle in the complex plane. This is illustrated in Figure 8, which shows the spectrum of a frame of seizure data and the zeros of P for a 12th order autoregressive fit to this

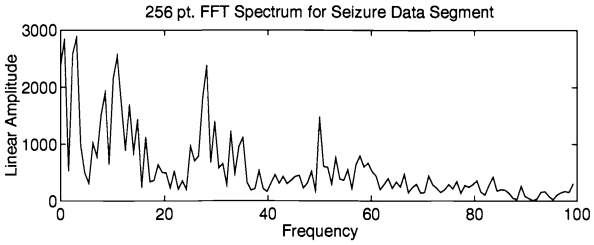

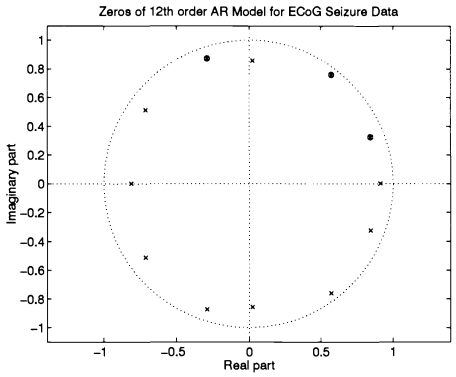

(a) (b)

Figure 8: ECoG Seizure Data Segment FFT Spectrum (a) and Corresponding AR Pole Plot (b)

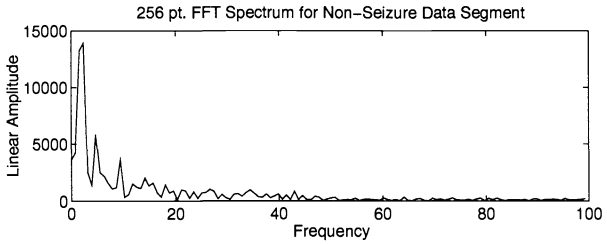

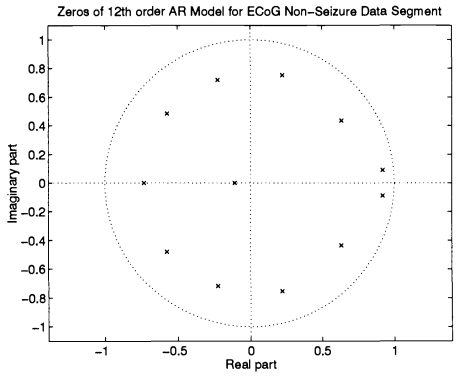

(a) (b)

Figure 9: ECoG Non-Seizure Data Segment FFT Spectrum (a) and Corresponding AR Pole Plot (b)

data. Figure 8(b) illustrates how the spectral peaks in the AR model are related to the zeros in close proximity to the unit circle. Ignoring the delta and theta wave activity (0-8 Hz), three strong spectral peaks can be found roughly at frequencies 12 Hz, 30 Hz, and 50 Hz in the seizure data of Figure 8. Given the fact that the AR model provides an approximation to the spectral characteristics of the data, these frequencies are consistent with frequencies identified earlier through WISP processing. For comparison, Figure 9 gives corresponding plots for a frame of non-seizure data, where the spectral peaks are noticeably absent.

For both seizure and non-seizure data, P has a single real zero near $z = 1$. This is due to the low frequency peak inherent to the spectrum of both the seizure and non-seizure data. Neglecting this zero, we find for the remaining zeros that:

(a) for seizure data, some zeros (usually three) are close to the unit circle;

(b) for non-seizure data, all zeros are well within the unit circle.

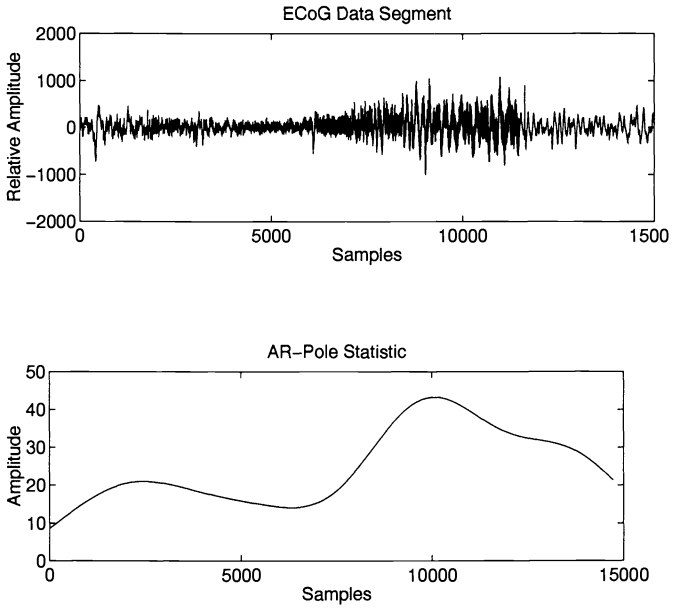

Figure 10: ECoG Data Segment (a) and Corresponding AR-Pole Statistic (b)

Based on these observations, we define the *AR Pole Statistic* A of a frame of data as follows. Suppose S is a family of subsets of the set of zeros of P. Define A by

$$A = \max_{C \in S} \sum_{r \in C} \frac{1}{1 - |r|} .$$

For our data, we find it useful to let S be the following family of subsets of zeros. C is a set in S if C has three zeros, each with argument θ satisfying $\pi/20 < \theta < \pi$. The normalized frequency $\pi/20$ corresponds to roughly 10 Hz as a minimal frequency and was selected after manual inspection of the ECoG data. Since the spectral content of the data x_n is dynamic, we generate a time series for the statistic A by letting A_n denote the statistic obtained from the autoregressive model derived from a frame of data F_n, referenced to index n. Figure 10 shows plots for x_n and A_n, where the ECoG data x_n contains both non-seizure and seizure intervals.

By smoothing the time series statistic A_n we obtain a reliable indicator for the presence of a seizure. It is interesting to note that the AR pole statistic begins to rise above its value for non-seizure areas during the electrodecremental period, as shown in Figure 10(a). Comparing the amplitude of the AR pole statistic in Figure 10(b) to the actual time series data in Figure 10(a), it is apparent that the statistic amplitude can be thresholded to indicate the first detection of spectral peaks (and hence seizure activity). If all available channels are processed with the AR pole statistic, localization can be performed by identifying that channel in which the AR pole statistic first exceeds a pre-set threshold.

5. SUMMARY OF RESULTS

Data from several patients have been analyzed using the techniques described in this paper. In each case, over 60 channels were examined (a few channels had unusable data), and each technique was able to provide a indication of dominant lines in the spectral characteristics of the data. In particular, the techniques appeared to be robust across different channels within a data segment (i.e., time epoch), different data segments for the same patient, and also different patients. Although the success of the individual techniques did vary from patient to patient, each methodology was able to identify seizure activity in channels where visual inspection of the waveforms was either nonexistent or weak.

6. CONCLUSIONS

In this paper, we showed that differences exist in the frequency spectrum structure of non-seizure and seizure ECoG data segments. The two processing techniques introduced here use this structural difference to distinguish between non-seizure and seizure states of ECoG data.

The wavelet based WISP technique uses a graphical scalogram representation to help identify the presence of narrowband frequency components. Thus far, it has been able to enhance the presence of weak line components that remain masked upon visual inspection of the time series or the frequency spectrum alone. The AR Pole statistic methodology computes a single statistic for each processing block that relates to change in frequency content between non-seizure and seizure data segments. Although the method can be used to identify particular frequencies, the statistic does not. Instead, this technique has been applied to identify general trends in dominant frequency activity, and in particular those that are related to changes in spectral shape relative to non-seizure and seizure activity.

Both methods are able to acurately detect the changes in the frequency spectrum as the seizure onset arrives. In most cases, the processing outputs depict the structural change before visual detection can be made. We feel that both of these techniquies can be used to help detect and localize seizure activity in ECoG recordings collected from epileptic patients.

7. ACKNOWLEDGMENT

The authors would like to gratefully acknowledge the support and medical expertise provided by both the doctors and technicians at the Children's National Medical Center in Washington, DC. In particular, we acknowledge Dr. Steven Schiff and Dr. Joan Conry for their technical support and guidance on medical and biological matters related to this paper. Furthermore, the data presented here was made available by Children's Hospital.

8. REFERENCES

1. R. Dorf, editor, The Electrical Engineering Handbook, CRC Press Inc., Boca Raton, FL, 1993.

2. P. Nunez, Electric Fields of the Brain: The Neurophysics of EEG, Oxford University Press, New York, 1981.

3. M. Bozek-Kuzmicki, D. Colella, G.M. Jacyna, "Feature-based epileptic seizure detection and prediction from ECoG recordings," International Symposium on Time-Frequency and Time-Scale Analysis, IEEE Signal Processing Society, pp. 564-567, Philadelphia, PA, 1994.

4. G. Benke, M. Bozek-Kuzmicki, D. Colella, "Early onset warning of epileptic seizures using an AR-based pole statistic," in preparation.